



Published in final edited form as:

*Leuk Lymphoma*. 2011 September ; 52(9): 1630–1640. doi:10.3109/10428194.2011.573036.

## Current and future imaging modalities for multiple myeloma and its precursor states

ESTHER TAN<sup>1,2</sup>, BRENDAN M. WEISS<sup>1,2</sup>, ESTHER MENA<sup>3</sup>, NEHA KORDE<sup>1</sup>, PETER L. CHOYKE<sup>3</sup>, and OLA LANDGREN<sup>1</sup>

<sup>1</sup>Multiple Myeloma Section, Medical Oncology Branch, Center for Cancer Research, National Cancer Institute, National Institutes of Health, Bethesda, MD, USA

<sup>2</sup>Hematology-Oncology Service, Department of Medicine, Walter Reed Army Medical Center, Washington, DC, USA

<sup>3</sup>Molecular Imaging Program, Center for Cancer Research, National Cancer Institute, National Institutes of Health, Bethesda, MD, USA

### Abstract

Traditionally, the skeletal survey has been the standard modality for the detection of osteolytic bone disease in multiple myeloma. In addition to its poor sensitivity for the detection of osteolytic lesions, this modality is not able to identify extramedullary lesions and focal bone marrow involvement, nor measure response to therapy. The application of novel imaging techniques such as computed tomography (CT), magnetic resonance imaging (MRI), and molecular imaging such as fluorine-18 fluorodeoxyglucose positron emission tomography CT (<sup>18</sup>F-FDG PET/CT) and fluorine-18 sodium fluoride positron emission tomography CT (<sup>18</sup>F-NaF PET/CT) has the potential to overcome these limitations as well as provide prognostic information in precursor states and multiple myeloma. Also promising is the use of dynamic contrast enhanced magnetic resonance imaging (DCE MRI) to measure vascular permeability, an important feature of myelomagenesis. This review summarizes the current status and possible future role of novel imaging modalities in multiple myeloma and its precursor states.

### Keywords

Multiple myeloma; monoclonal gammopathy of undetermined significance; smoldering multiple myeloma; skeletal survey; PET/CT; DCE MRI

### Case report

The patient is a previously healthy 54-year-old Caucasian male who experienced severe left arm pain while lifting a heavy bag at an airport. Plain radiographs revealed a left humeral fracture (Figure 1). The patient was then placed in a sling for 4 weeks. During this time, he developed numbness and tingling of his right arm, prompting further imaging.

© 2011 Informa UK, Ltd.

Correspondence: Dr. Esther Tan, Walter Reed Army Medical Center, 6900 Georgia Avenue, Washington, DC 20307, USA. Tel: +1-202-782-4950. Fax: +1-202-782-3256. esther.tan@us.army.mil. Dr. Ola Landgren, Multiple Myeloma Section, Medical Oncology Branch, Center for Cancer Research, National Cancer Institute, National Institutes of Health, 9000 Rockville Pike, Bldg 10/Room 13N240, Bethesda, MD 20892, USA. Tel: +1-301-496-0670. Fax: +1-301-402-0172. landgreo@mail.nih.gov.

**Potential conflict of interest:** Disclosure forms provided by the authors are available with the full text of this article at [www.informahhealthcare.com/lal](http://www.informahhealthcare.com/lal).

Magnetic resonance imaging (MRI) of his spine revealed a T1 destructive lesion with epidural extension from C7 to T1 (Figure 2). Further laboratory evaluation revealed an immunoglobulin G (IgG)  $\kappa$  monoclonal protein of 1.6 g/dL on serum protein electrophoresis (SPEP), hemoglobin of 10 g/dL, creatinine of 0.99 mg/dL, albumin of 3.2 g/dL, calcium of 2.25 mmol/L, and a  $\beta_2$ -microglobulin of 2.7 mg/L. His serum free light chain (FLC) ratio was also abnormal at 32 ( $\kappa$  =61 mg/dL;  $\lambda$  =1.88 mg/dL).

He later underwent a left humeral internal fixation. Biopsies obtained from both the T1 lesion and the left proximal humerus were consistent with a plasma cell neoplasm, as determined by CD138-positive kappa restricted plasma cells. His bone marrow biopsy demonstrated 5–10% CD138 plasma cells with aberrant expression of CD56. In addition, a fluorine-18 fluorodeoxyglucose positron emission tomography/computed tomography ( $^{18}\text{F}$ -FDG PET/CT) scan revealed additional bone marrow lesions at the left transverse process of T10, the body of L3, left posterior scapula, left inferior sacrum, and the left femur (Figure 3), not previously seen on a skeletal survey.

The constellation of imaging findings, pathology reports, and laboratory values led to the diagnosis of multiple myeloma with an International Staging System (ISS) score of 2. The patient received radiation therapy to the T1 lesion, left humerus, and left sacrum with improvement of his pain and neurologic symptoms. He is currently on systemic therapy with lenalidomide, bortezomib, and low dose dexamethasone.

## Introduction

Multiple myeloma is a malignant plasma cell disorder and is the second most common hematologic malignancy in the United States, with about 20 000 patients diagnosed annually [1]. According to current diagnostic criteria, multiple myeloma is diagnosed in the presence of a monoclonal protein detectable in the blood or urine, light chain restricted plasma cells in the bone marrow, and myeloma-related end-organ damage [2]. The features of end-organ damage are defined as follows: hypercalcemia, renal insufficiency, anemia, and/or bone disease manifested by osteolytic lesions or osteoporosis. Osteolytic lesions are most commonly found in the axial skeleton, skull, shoulder girdle, proximal humeri, ribs, and proximal femurs [3]. Additionally, patients may present with multiple extramedullary plasmacytomas at diverse sites, including the nasopharynx, larynx, and upper respiratory tract [4].

The above case report illustrates the limitations of current imaging techniques in multiple myeloma, based predominantly on the findings of skeletal survey. The use of more sensitive imaging modalities, in this case MRI and PET, were able to render a diagnosis and alter clinical management even though the patient had low monoclonal protein levels and a low plasma cell burden in his bone marrow. This highlights the complementary role these additional imaging modalities have in the management of multiple myeloma.

## Limitations of the skeletal survey in multiple myeloma

Traditionally, the skeletal survey has been the gold standard imaging modality to detect osteolytic lesions [5]. The skeletal survey is a series of plain films that include the chest, skull, humeri, femora, and pelvis as well as anteroposterior and lateral images of the whole spine. Information regarding the presence of lytic bone lesions was incorporated into the Durie–Salmon staging system, which was developed over 30 years ago [6]. However, the skeletal survey is insensitive for the detection of osteolytic lesions as it requires at least 30% cortical bone destruction [7]. Because the skeletal survey requires 20 separate films, the patient typically spends a lengthy period of time on the radiographic table. This may be an

important issue for those patients with severe pain as they are rotated and positioned for multiple radiographic images [5].

It is also difficult to quantify (including linear measurements) plain radiographs due to magnification changes. Furthermore, the skeletal survey cannot be used to assess response, as osteolytic lesions may not change radiographically following therapy. Because of the multiple limitations of the skeletal survey, there is increasing interest in improving imaging techniques in multiple myeloma. Features of an optimal imaging technique include high sensitivity for detecting lytic bone lesions as well as infiltrative focal lesions in the bone marrow, reliable detection of extramedullary disease, and being able to assess response to treatment (Table I).

### Improved detection of osteolytic lesions in multiple myeloma

Multidetector computed tomography (MDCT) has been used in the detection of osteolytic lesions in multiple myeloma because it allows for whole body imaging and excellent anatomic detail. Mahnken *et al.* studied the utility of MDCT in 18 patients with Durie–Salmon stage III multiple myeloma and compared the findings with those of the skeletal survey [8]. In the 18 patients, a total of 325 vertebrae were examined. Their findings showed that the skeletal survey detected bone lesions in 207 vertebrae, compared to 231 vertebral lesions detected by MDCT. Importantly, MDCT detected twice as many lesions at risk of fracture, compared to the skeletal survey (12 vs. 6), defined as lytic lesions with >50% volume loss.

A major disadvantage of MDCT, however, is high radiation doses (>35 mSv). An alternative approach is the use of low dose CT (LDCT) where the average dose is about 3.3 mSv. Gleeson and colleagues tested LDCT's feasibility in diagnosing and staging patients with multiple myeloma [9]. In their study, 34 patients with biopsy-confirmed multiple myeloma and five with monoclonal gammopathy of undetermined significance (MGUS) or smoldering multiple myeloma (SMM) were enrolled. All patients underwent LDCT and a skeletal survey. LDCT was found to detect more osteolytic lesions, allowing the restaging of 25 cases (20 cases were upstaged) using the Durie–Salmon PLUS staging system. One patient was also found to have a clinically important lesion in the vertebral body with erosion into the spinal canal, detected by LDCT but not the skeletal survey. This patient subsequently required urgent radiation therapy.

These two studies show that computed tomography (whether high dose or low dose) appears to be superior to the skeletal survey for the detection of osteolytic lesions. Detection of these additional lesions has the potential to alter clinical management.

Another area of great interest is the fusion of anatomic imaging (CT) with functional imaging (PET). Functional imaging using  $^{18}\text{F}$ -FDG PET allows the detection of malignant plasma cells because  $^{18}\text{F}$ -FDG is trapped in the cells after being taken up via GLUT1 glucose transporters, since it is not recognized by the hexose monophosphatases and therefore not further metabolized [10]. When PET scan results are combined with imaging obtained from low dose CT ( $^{18}\text{F}$ -FDG PET/CT), the presence of osteolytic lesions, focal lesions in the bone marrow, and extramedullary disease can be detected [11].

When  $^{18}\text{F}$ -FDG PET/CT was compared to the skeletal survey, Nanni *et al.* found a higher number of lesions in 16 out of 28 patients with newly diagnosed symptomatic myeloma [12]. In nine of the 16 patients, the skeletal survey was completely normal, while  $^{18}\text{F}$ -FDG PET/CT detected one or more lytic bone lesions. They also found that  $^{18}\text{F}$ -FDG PET/CT detected a second bone lesion in a patient who was originally thought to have a solitary plasmacytoma, changing the diagnosis to multiple myeloma. Other studies have calculated a

sensitivity range of 80–90% and a specificity range of 80–100% of  $^{18}\text{F}$ -FDG PET/CT in detecting osteolytic lesions in multiple myeloma [13,14].

Because of the lack of osteoblastic response to lytic lesions, bone scintigraphy has a limited role in the staging of patients with multiple myeloma. Its sensitivity in detecting multiple myeloma bone disease was found to range between 40 and 60% [15]. When Ludwig *et al.* compared bone scintigraphy to the skeletal survey in multiple myeloma, they found that radionuclide imaging was inferior to conventional X-rays in the detection of bone lesions [15]. This is in contrast to  $^{18}\text{F}$ -NaF PET/CT, which was found to be sensitive to both osteoblastic as well as osteolytic lesions [16]. Increased  $^{18}\text{F}$ -fluoride uptake was found at the periphery of these lytic lesions [16]. When combined with LDCT, the specificity of  $^{18}\text{F}$ -NaF PET increases, allowing it to distinguish benign lesions from malignant ones. Further studies are required to investigate the utility of  $^{18}\text{F}$ -NaF PET/CT in the detection of myelomatous bone disease.

### Techniques to improve detection of infiltrative focal bone marrow disease

Although whole body magnetic resonance imaging (WB-MRI) is inferior to MDCT when it comes to detecting bony lesions, its strength lies in its ability to image the bone marrow directly and to detect the pattern and extent of bone marrow infiltration in the absence of osteolytic lesions [17]. Unlike conventional MRI, WB-MRI enables an expanded field of view, encompassing all or nearly all of the body. WB-MRI works by obtaining imaging of multiple sections of the body and ‘stitching’ them together electronically. Dinter *et al.* studied WB-MRI and its role in detecting focal and diffuse infiltrative bone marrow lesions [18]. In 60 patients with multiple myeloma, the entire axial skeletal was imaged with both WB-MRI and conventional radiography. They also looked at the influence of WB-MRI on therapeutic decisions. They found that WB-MRI revealed additional areas of abnormalities, and the most significant area of discordance between the two studies was the detection of diffuse disease infiltration on the WB-MRI, which was not detectable on the skeletal survey. Thus, 41 out of 60 (68%) patients had their disease stage upgraded using the Durie–Salmon PLUS staging system by the WB-MRI. When they looked at the group of patients requiring further therapy (24 out of 60 patients), the WB-MRI was the most important factor in 10 out of the 24 patients in prompting the initiation of further therapy because it detected extramedullary lesions in six of the 10 patients and impending fractures in three patients.

Moreover, Walker *et al.* conducted a prospective study in 668 patients with multiple myeloma using pre- and post-treatment imaging evaluations with both a skeletal survey and an MRI of the axial bone marrow [19]. They found that MRI detected focal lesions in 139 patients who had normal skeletal surveys. CT-guided fine needle aspiration (FNA) of the MRI focal lesions confirmed focal osteolysis in 97% of these patients. They also found that MRI had a higher sensitivity in the spine, sternum, and pelvis. Their data led them to conclude that MRI should be used to complement the skeletal survey in assessing patients with multiple myeloma because it allows the detection of bone marrow focal lesions before osteolytic lesions are seen on the skeletal survey [19].

Another technique that has been used to detect focal infiltrative bone marrow lesions is technetium-99-m labeled hexakis-2-methoxy-isobutyl-isonitrite ( $^{99\text{m}}\text{Tc}$ -sestamibi). This tracer was initially introduced as a myocardial perfusion agent, where it is still commonly used [20,21]. Because of its propensity to accumulate in tissues with high cell density and mitochondrial activation,  $^{99\text{m}}\text{Tc}$ -sestamibi has also been used to study malignant tumors [22]. Various studies have also reported uptake of this tracer by myeloma cells [23–25]. One such study was conducted by Pace *et al.*, where 39 patients with multiple myeloma (29 with active disease and 10 in remission) underwent  $^{99\text{m}}\text{Tc}$ -sestamibi scans [23]. Each scan was

classified as normal, diffuse uptake, focal uptake, or diffuse and focal uptake. The scans with diffuse uptake were further characterized in terms of the intensity of the uptake. In the results, they found 32 abnormal scans and seven normal scans. All the normal scans were found in patients in remission after chemotherapy, while 91% of the abnormal scans were in patients with active disease. They also found that patients with low-burden disease had scans with low-intensity diffuse uptake, while those with a higher-stage disease had focal uptake or high-intensity diffuse uptake. The authors concluded that  $^{99m}\text{Tc}$ -sestamibi was a potentially useful technique in the detection of myeloma in the bone marrow, and that the type and intensity of uptake correlated with disease severity.

Although it is used mainly in the study of brain tumors, investigators have also found that increased  $^{11}\text{C}$ -methionine uptake may represent abnormal myeloma cells that are producing immunoglobulins. In a prospective study, Dankerl *et al.* imaged 19 patients with active multiple myeloma (13 were untreated) versus 10 controls with  $^{11}\text{C}$ -methionine PET/CT [26]. In their study, they found that all the control patients had low  $^{11}\text{C}$ -methionine bone marrow uptake in the bone marrow space of T11 (maximum mean standard uptake value [ $\text{SUV}_{\text{max}}$ ] =  $1.8 \pm 0.3$ ) as compared to visually normal bone marrow of patients with multiple myeloma (treated: mean  $\text{SUV}_{\text{max}}$  =  $4.3 \pm 2$ ; untreated: mean  $\text{SUV}_{\text{max}}$  =  $4.6 \pm 2.9$ ). All 13 of the untreated patients with multiple myeloma were found to have multiple focal bone marrow lesions. While some of these lesions corresponded to findings on the LDCT, others were without any structural changes. From their findings, the authors speculated that  $^{11}\text{C}$ -methionine PET/CT has the potential to play a role in detecting early bone changes, estimating tumor burden, as well as complementing the stage classification of multiple myeloma [26].

## Imaging to assess treatment response in multiple myeloma

Response to treatment in multiple myeloma is currently measured by laboratory parameters, which include serum protein electrophoresis, urine protein electrophoresis, bone marrow evaluation, and serum free light chains [27]. Because conventional radiographs do not allow the assessment of extramedullary disease or focal bone marrow disease, radiographic response assessment looking at these two characteristics of the disease is limited. Myeloma-induced bone lesions also seldom heal, even with therapy, as bisphosphonates and immunomodulatory agents do not affect the activity of the osteoblasts [28]. Therefore, the skeletal survey is not able to assess for treatment response in patients with multiple myeloma.

Recently, however, the Arkansas group has reported the largest and most comprehensive study on the impact of imaging in treatment response in multiple myeloma when undergoing the Total Therapy 3 therapeutic program (an intensive multiagent induction chemotherapy and tandem autologous stem cell transplant regimen followed by maintenance therapy for 3 years) [29]. All patients had a skeletal survey, MRI, and  $^{18}\text{F}$ -FDG PET/CT at baseline and at specified points in their protocol. Complete  $^{18}\text{F}$ -FDG suppression in both focal lesions and extramedullary lesions in PET before transplant conferred superior overall and event-free survival at 30 months. Other studies have also shown that post-treatment declines of  $^{18}\text{F}$ -FDG PET/CT activity have been associated with clinical improvement, as well as a positive response to treatment [30,31].

$^{99m}\text{Tc}$ -sestamibi is another imaging method that may be used in the follow-up of patients with multiple myeloma. Mele *et al.* sought not only to compare it with the skeletal survey in the staging of patients with multiple myeloma but also to evaluate its usefulness post-treatment [32]. In their study, 229 scans were obtained at baseline while 168 were obtained at follow-up. The majority of the patients who had follow-up scans had multiple myeloma



(91%), while the rest had solitary plasmacytoma. In their results, they found that 86% of their patients who had a complete response to treatment had negative scans, while 73% of those who had minimal response had positive scans. All patients with no response to treatment had positive scans. In this study, they also found a positive correlation between the scans and clinical and biological parameters that indicated tumor burden and disease activity.

Imaging with dynamic contrast enhanced MRI (DCE MRI) can also be used to assess response to treatment in multiple myeloma. DCE MRI is a non-invasive technique that can detect vascular permeability in malignant tissues [33]. It involves the serial acquisition of MR images of a tissue of interest before, during, and after the injection of a gadolinium chelate. After the signal is converted into gadolinium concentration, the signal intensity curve can be fitted to a two-compartment pharmacokinetic model from which parameters such as the rate constants,  $K_{trans}$  and  $K_{ep}$ , can be derived. These parameters have complex physiologic meaning but can be used to serially assess response to angiogenic inhibitors [34].

Lin *et al.* performed DCE MRI pre- and post-treatment in 30 patients with multiple myeloma [35]. Twenty patients received induction therapy followed by high dose therapy and an autologous stem cell transplant, while 30 received only induction therapy. Parameters assessed included MR pattern of bone marrow infiltration, size of focal lesions, bone marrow enhancement percentage based on time–signal intensity curves, and focal lesion enhancement percentage. Post-treatment changes in these parameters were compared with clinical response to treatment. Patients were labeled as good responders if they achieved a complete response (CR) or a very good partial response (VGPR) defined by laboratory criteria, and poor responders if they achieved a partial response, had stable disease, or had progressive disease. Their results show that the good responders had significantly less percent bone marrow enhancement compared with the pre-treatment bone marrow. These patients also had a change in the timing of focal lesion enhancement. Before treatment, the focal lesions showed early enhancement, but after induction chemotherapy, good responders showed a delay in the peak enhancement. Lin *et al.* concluded that DCE MRI can be used to assess response in patients who have received systemic chemotherapy as well as early detection of disease progression after high dose therapy. They also noted that DCE MRI could potentially be used to assess response in patients with oligo- or non-secretory myeloma.

## Imaging to improve prognostic assessment in multiple myeloma

The ISS staging system, the Durie–Salmon staging system, and the Durie–Salmon PLUS staging system are three systems for assessing prognosis in multiple myeloma [6,36–38]. These systems rely largely on clinical and laboratory findings and not anatomic details from imaging studies. The Durie–Salmon PLUS staging system, although not in wide use, has incorporated novel imaging techniques. In this system, poor-risk patients have greater than 20 lesions and/or extramedullary lesions found on MRI or  $^{18}\text{F}$ -FDG PET/CT. In addition, prognosis in multiple myeloma can be assessed through the use of molecular features that confer high risk, such as fluorescence *in situ* hybridization (FISH) for t(4;14), t(14;16), t(14;20), and del17p, aneuploidy, and deletion 13 on metaphase cytogenetics [39].

Kusumoto *et al.* presented one of the earliest studies that showed that abnormal MRI patterns (diffuse or nodular) correlated to inferior survival [40]. In their prospective study, 61 patients with multiple myeloma had MRI studies along with baseline laboratory parameters. These patients were then followed for 1–73 months. The majority of the patients ( $n=53$ ) received treatment with melphalan and prednisolone, VAD (vincristine, adriamycin,

and dexamethasone), or VCAP (vincristine, cyclophosphamide, adriamycin, and prednisone). Patients with a normal MRI pattern had a significantly longer 5-year survival rate of 80%, compared to 30% in those with an abnormal pattern. The patients with nodular and diffuse MRI pattern were also found to have the worst survival among those with abnormal MRI patterns.

Moulopoulos *et al.* also showed that patients with diffuse marrow replacement on MRI had a poorer prognosis [41]. In their study, 142 patients with multiple myeloma obtained pre-treatment imaging with an MRI of the thoracic and lumbar spine. In their group of patients, 50% were found to have focal marrow lesions, 28% had a diffuse pattern, 14% had a variegated pattern, and 8% were normal. All patients then proceeded to receive treatment with vincristine/doxorubicin/dexamethasone, melphalan/dexamethasone, VAD bolus, or VAD with liposomal doxorubicin, and the hyper-CVAD (hyperfractionated cyclophosphamide/vincristine/doxorubicin/dexamethasone) regimen. High dose therapy with autologous stem cell transplant was administered to 61 patients. Survival was calculated from the start of treatment to death or the last follow-up visit. They found that patients with a pre-treatment diffuse pattern on their MRI of the bone marrow had a median survival of 24 months, compared to 56 months in those with a normal pattern ( $p < 0.001$ ).

In a more recent study, Castellani *et al.* performed  $^{18}\text{F}$ -FDG PET in 18 patients with a recent diagnosis of multiple myeloma prior to treatment [42]. All patients underwent standard chemotherapy at the time of diagnosis. Mean follow-up was 43 months. Patients were then divided into two groups based on their outcome: group A had patients with rapid progression of multiple myeloma and group B had patients with less aggressive disease. When they looked at the mean SUV of two regions of interest positioned on both femora whose bone marrow was visible on coronal slices, they found higher values in patients with the more aggressive disease (group A). A univariate regression analysis showed that the mean SUV was also linearly related to survival in their patients.

To our knowledge, the first systematic study looking at prognosis using DCE MRI and multiple myeloma was conducted by Hillengass *et al.* [43]. In their study, 60 patients with progressive or relapsed multiple myeloma and five newly diagnosed patients had a DCE MRI prior to further therapy with a thalidomide based therapy. They then followed these patients for a median of 56 months. During follow-up, 47 patients had progressive disease. The median overall survival was 49.5 months. Using a multivariate Cox model, DCE MRI parameters along with other factors ( $\beta_2$ -microglobulin [B2M], albumin, lactate dehydrogenase [LDH]) were investigated. They found that one MRI parameter, amplitude A, a measure of vascular permeability, and B2M were independent prognostic factors for event-free survival, with B2M being the sole predictor of overall survival. The authors concluded that abnormal amplitude A likely reflects an increase in micro-circulation, which correlates to disease activity. They also mentioned that DCE MRI may play an important role in the future in identifying patients who could benefit most from anti-angiogenic drugs.

## Imaging to improve prognostic assessment in patients with monoclonal gammopathy of undetermined significance and smoldering multiple myeloma

Multiple myeloma is consistently preceded by a pre-malignant state, MGUS or SMM [44,45]. In MGUS, patients have a monoclonal protein spike less than 3 g/dL, and per definition they have less than 10% plasmacytosis in the bone marrow and no end-organ damage [2]. SMM is defined by 3 g/dL or greater of monoclonal protein in the blood and/or 10% or greater plasmacytosis in the bone marrow, in the absence of end-organ damage [2].

The average risk of progression to multiple myeloma is approximately 1% per year for patients with MGUS and 10% per year for patients with SMM [46,47]. However, the actual risk of multiple myeloma progression for individual patients with MGUS/SMM varies greatly [48].

Currently, we lack biological predictors for the progression from MGUS/SMM to multiple myeloma. One proposed hypothesis to explain the transition from pre-malignant to malignant states is the presence of an ‘angiogenic switch,’ resulting in the imbalance of pro- and anti-angiogenic factors, creating a pro-angiogenic environment that supports tumor growth [49]. Rajkumar *et al.* evaluated angiogenesis in 400 patients with MGUS, SMM, multiple myeloma, and AL amyloidosis [50]. Using CD34 immunohistochemical staining to detect bone marrow microvessels, high grade microvessel density was seen in 1% of patients with MGUS, 3% of patients with SMM, 29% of patients with newly diagnosed multiple myeloma, and 42% of patients with relapsed multiple myeloma. Several studies have also shown that increased angiogenesis is an adverse prognostic marker for patients with multiple myeloma [51–54]. However, determination of angiogenic grade from biopsy samples is limited by the invasiveness of the procedure, because it is anatomic and not physiologic, and because it provides only a small sample of one part of the bone marrow.

Moulopoulos *et al.* obtained MRI of the thoracic and lumbosacral spine in 38 patients with newly diagnosed SMM [55]. In 19 of these patients, the MRI studies were found to be normal, while the others had variegated, diffuse, or focal patterns. These patients were then followed every 2 months. Moulopoulos *et al.* found that the median time to progression to multiple myeloma for all patients was 29 months. However, when the groups were divided into normal and abnormal MRI studies, they found that the median time to progression was far longer in the patients with normal MRIs versus abnormal MRIs (43 months vs. 16 months). Therefore, the authors concluded that abnormal MRI patterns in patients with SMM may provide the justification to start treatment. When 24 patients with MGUS underwent MRI of the thoracolumbar spine, Bellaiche *et al.* found that all patients had normal scans, compared to only 86% of patients with SMM [56].

One of the first studies to report the utility of <sup>18</sup>F-FDG PET in patients with MGUS was reported by Durie *et al.* [57]. In this retrospective study of patients imaged between 1996 and 2000, all patients with active multiple myeloma had an abnormal PET scan despite 25% with negative skeletal survey. All patients with MGUS, however, who were followed between 3 and 43 months, had negative scans.

Hillengass *et al.* evaluated DCE MRI of the lumbar spine in 222 patients with MGUS, SMM, and multiple myeloma and 22 healthy controls [58]. They found statistically significant abnormal rate constants between normal controls and those with SMM and between normal controls and those with multiple myeloma, with a higher difference in value between the normal controls and those with multiple myeloma. They also found a correlation between the DCE MRI peak intensity and bone marrow plasmacytosis. Although their study did not allow for complete patient follow-up, one of their asymptomatic patients with a diffuse variant (a pattern of increased microcirculation) DCE MRI developed multiple myeloma 6 months after the study [58]. The authors proposed that DCE MRI can be used to recognize patients at higher risk for progression and that these patients should be considered for the initiation of early therapy.

### **Brief comment on costs of novel imaging modalities**

Without any doubt, novel imaging modalities have a significantly higher sensitivity than conventional X-rays. Based on the Medicare reimbursement rate in the United States, the cost of a skeletal survey is approximately \$US100, compared to the cost of CT of the chest,



abdomen, and pelvis of about \$US1000 [59]. When combined with PET, the cost of PET/CT can run anywhere from \$US1000 to \$US4000, depending on the tracer and the body part that is being imaged. As for MRI of the L spine, reimbursement rates are estimated around \$US500. If a patient were to receive PET/CT and MRI of the L spine, the total cost could come to approximately \$US1500–\$US4500. At the same time, however, the cost of induction therapy with novel agents such as lenalidomide and bortezomib has been estimated at \$US10 000 per cycle. Since most therapy with multiple myeloma will require at least four cycles, the total cost for induction therapy is at least \$US40 000.

## Clinical management based on current knowledge regarding novel imaging modalities

At this time, clinical guidelines do not mandate the use of novel imaging modalities in patients with MGUS, SMM, and multiple myeloma. We also do not know to what extent these techniques will improve or change existing clinical practice and/or therapeutic decisions. It is possible that abnormal imaging findings may prompt a clinician to initiate therapy sooner rather than later, or to decrease the surveillance interval of such patients. At our institution, we are currently investigating the feasibility of these techniques in patients with MGUS, SMM, and multiple myeloma. Our results so far have been promising. For example, we have upgraded some patients with high-risk SMM to multiple myeloma because  $^{18}\text{F}$ -FDG PET/CT detected lytic lesions not identified in the skeletal survey. Our preliminary results show that patients with MGUS have no clinically significant abnormalities detectable by  $^{18}\text{F}$ -FDG PET/CT,  $^{18}\text{F}$ -NaF PET/CT, and DCE MRI of the lumbar spine.

We will need further studies to determine what role these new imaging techniques will play in the detection of residual disease and the current response criteria in multiple myeloma. It would be interesting to compare response via laboratory parameters such as flow cytometry and free light chain ratio to the response seen on these novel imaging modalities.

## Summary and conclusions

It is now generally acknowledged that the current gold standard imaging modality in multiple myeloma, the skeletal survey, has limited sensitivity and specificity for detecting myeloma-related osteolytic lesions. Since the diagnosis of multiple myeloma is dependent on the diagnosis of end-organ damage, better, more sensitive techniques are needed to replace the skeletal survey. Clearly, the introduction of novel imaging techniques such as CT, PET/CT, and MRI has improved the detection of myeloma lesions (Table II). These techniques may also play an important role in the assessment of treatment response as well as give important prognostic information.

Prior studies have also suggested that angiogenesis plays a role in the progression of pre-myeloma conditions to overt multiple myeloma [49,53]. Since DCE MRI is a novel technique that can assess angiogenesis in the bone marrow, future studies are needed to investigate whether it can reliably predict progression to multiple myeloma as well as response to treatment.

## Acknowledgments

These views are those of the authors and should not be taken as official views of the Department of Defense or the US Government.

## References

1. Jemal A, Siegel R, Ward E, et al. Cancer statistics, 2008. *CA Cancer J Clin.* 2008; 58:71–96. [PubMed: 18287387]
2. Criteria for the classification of monoclonal gammopathies, multiple myeloma and related disorders: a report of the International Myeloma Working Group. *Br J Haematol.* 2003; 121:749–757. [PubMed: 12780789]
3. Shortt CP, Carty F, Murray JG. The role of whole-body imaging in the diagnosis, staging, and follow-up of multiple myeloma. *Semin Musculoskelet Radiol.* 2010; 14:37–46. [PubMed: 20229439]
4. Winterbottom AP, Shaw AS. Imaging patients with myeloma. *Clin Radiol.* 2009; 64:1–11. [PubMed: 19070692]
5. Dimopoulos M, Terpos E, Comenzo RL, et al. International myeloma working group consensus statement and guidelines regarding the current role of imaging techniques in the diagnosis and monitoring of multiple myeloma. *Leukemia.* 2009; 23:1545–1556. [PubMed: 19421229]
6. Durie BG, Salmon SE. A clinical staging system for multiple myeloma. Correlation of measured myeloma cell mass with presenting clinical features, response to treatment, and survival. *Cancer.* 1975; 36:842–854. [PubMed: 1182674]
7. Edelstyn GA, Gillespie PJ, Grebbell FS. The radiological demonstration of osseous metastases. Experimental observations. *Clin Radiol.* 1967; 18:158–162. [PubMed: 6023348]
8. Mahnken AH, Wildberger JE, Gehbauer G, et al. Multi-detector CT of the spine in multiple myeloma: comparison with MR imaging and radiography. *AJR Am J Roentgenol.* 2002; 178:1429–1436. [PubMed: 12034612]
9. Gleeson TG, Moriarty J, Shortt CP, et al. Accuracy of whole-body low-dose multidetector CT (WBLDCT) versus skeletal survey in the detection of myelomatous lesions, and correlation of disease distribution with whole-body MRI (WBMRI). *Skeletal Radiol.* 2009; 38:225–236. [PubMed: 19009290]
10. Juweid ME, Cheson BD. Positron-emission tomography and assessment of cancer therapy. *N Engl J Med.* 2006; 354:496–507. [PubMed: 16452561]
11. Breyer RJ 3rd, Mulligan ME, Smith SE, et al. Comparison of imaging with FDG PET/CT with other imaging modalities in myeloma. *Skeletal Radiol.* 2006; 35:632–640. [PubMed: 16758246]
12. Nanni C, Zamagni E, Farsad M, et al. Role of 18F-FDG PET/CT in the assessment of bone involvement in newly diagnosed multiple myeloma: preliminary results. *Eur J Nucl Med Mol Imaging.* 2006; 33:525–531. [PubMed: 16453155]
13. Schirrmeyer H, Bommer M, Buck AK, et al. Initial results in the assessment of multiple myeloma using 18F-FDG PET. *Eur J Nucl Med Mol Imaging.* 2002; 29:361–366. [PubMed: 12002711]
14. Bredella MA, Steinbach L, Caputo G, et al. Value of FDG PET in the assessment of patients with multiple myeloma. *AJR Am J Roentgenol.* 2005; 184:1199–1204. [PubMed: 15788594]
15. Ludwig H, Kumpan W, Sinzinger H. Radiography and bone scintigraphy in multiple myeloma: a comparative analysis. *Br J Radiol.* 1982; 55:173–181. [PubMed: 7066617]
16. Even-Sapir E, Mishani E, Flusser G, et al. 18F-Fluoride positron emission tomography and positron emission tomography/computed tomography. *Semin Nucl Med.* 2007; 37:462–469. [PubMed: 17920353]
17. Angtuaco EJ, Fassas AB, Walker R, et al. Multiple myeloma: clinical review and diagnostic imaging. *Radiology.* 2004; 231:11–23. [PubMed: 14990813]
18. Dinter DJ, Neff WK, Klaus J, et al. Comparison of whole-body MR imaging and conventional X-ray examination in patients with multiple myeloma and implications for therapy. *Ann Hematol.* 2009; 88:457–464. [PubMed: 18941746]
19. Walker R, Barlogie B, Haessler J, et al. Magnetic resonance imaging in multiple myeloma: diagnostic and clinical implications. *J Clin Oncol.* 2007; 25:1121–1128. [PubMed: 17296972]
20. Ak I, Aslan V, Vardareli E, et al. Tc-99m methoxyisobutylisonitrile bone marrow imaging for predicting the levels of myeloma cells in bone marrow in multiple myeloma: correlation with CD38/CD138 expressing myeloma cells. *Ann Hematol.* 2003; 82:88–92. [PubMed: 12601486]

21. Lette J, Cerino M, Demaria S, et al. Serendipitous diagnosis of multiple myeloma during sestamibi myocardial perfusion imaging. *Clin Nucl Med*. 2002; 27:832–833. [PubMed: 12394147]
22. Maffioli L, Steens J, Pauwels E, et al. Applications of <sup>99m</sup>Tc-sestamibi in oncology. *Tumori*. 1996; 82:12–21. [PubMed: 8623497]
23. Pace L, Catalano L, Pinto A, et al. Different patterns of technetium-99m sestamibi uptake in multiple myeloma. *Eur J Nucl Med*. 1998; 25:714–720. [PubMed: 9662593]
24. Catalano L, Pace L, Califano C, et al. Detection of focal myeloma lesions by technetium-99m-sestaMIBI scintigraphy. *Haematologica*. 1999; 84:119–124. [PubMed: 10091409]
25. Adams BK, Fataar A, Nizami MA. Technetium-99m-sestamibi uptake in myeloma. *J Nucl Med*. 1996; 37:1001–1002. [PubMed: 8683291]
26. Dankerl A, Liebisch P, Glatting G, et al. Multiple myeloma: molecular imaging with <sup>11</sup>C-methionine PET/CT—initial experience. *Radiology*. 2007; 242:498–508. [PubMed: 17179397]
27. Durie BG, Harousseau JL, Miguel JS, et al. International uniform response criteria for multiple myeloma. *Leukemia*. 2006; 20:1467–1473. [PubMed: 16855634]
28. Terpos E, Dimopoulos MA, Sezer O. The effect of novel anti-myeloma agents on bone metabolism of patients with multiple myeloma. *Leukemia*. 2007; 21:1875–1884. [PubMed: 17611556]
29. Bartel TB, Haessler J, Brown TL, et al. F18-fluorodeoxyglucose positron emission tomography in the context of other imaging techniques and prognostic factors in multiple myeloma. *Blood*. 2009; 114:2068–2076. [PubMed: 19443657]
30. Jadvar H, Conti PS. Diagnostic utility of FDG PET in multiple myeloma. *Skeletal Radiol*. 2002; 31:690–694. [PubMed: 12483429]
31. Zamagni E, Nanni C, Patriarca F, et al. A prospective comparison of <sup>18</sup>F-fluorodeoxyglucose positron emission tomography-computed tomography, magnetic resonance imaging and whole-body planar radiographs in the assessment of bone disease in newly diagnosed multiple myeloma. *Haematologica*. 2007; 92:50–55. [PubMed: 17229635]
32. Mele A, Offidani M, Visani G, et al. Technetium-99m sestamibi scintigraphy is sensitive and specific for the staging and the follow-up of patients with multiple myeloma: a multicentre study on 397 scans. *Br J Haematol*. 2007; 136:729–735. [PubMed: 17233770]
33. Choyke PL, Dwyer AJ, Knopp MV. Functional tumor imaging with dynamic contrast-enhanced magnetic resonance imaging. *J Magn Reson Imaging*. 2003; 17:509–520. [PubMed: 12720260]
34. Brix G, Semmler W, Port R, et al. Pharmacokinetic parameters in CNS Gd-DTPA enhanced MR imaging. *J Comput Assist Tomogr*. 1991; 15:621–628. [PubMed: 2061479]
35. Lin C, Luciani A, Belhadj K, et al. Multiple myeloma treatment response assessment with whole-body dynamic contrast-enhanced MR imaging. *Radiology*. 2010; 254:521–531. [PubMed: 20093523]
36. Greipp PR, San Miguel J, Durie BG, et al. International staging system for multiple myeloma. *J Clin Oncol*. 2005; 23:3412–3420. [PubMed: 15809451]
37. Bataille R, Durie BG, Grenier J, et al. Prognostic factors and staging in multiple myeloma: a reappraisal. *J Clin Oncol*. 1986; 4:80–87. [PubMed: 3510284]
38. Durie BG. The role of anatomic and functional staging in myeloma: description of Durie/Salmon plus staging system. *Eur J Cancer*. 2006; 42:1539–1543. [PubMed: 16777405]
39. Stewart AK, Bergsagel PL, Greipp PR, et al. A practical guide to defining high-risk myeloma for clinical trials, patient counseling and choice of therapy. *Leukemia*. 2007; 21:529–534. [PubMed: 17230230]
40. Kusumoto S, Jinnai I, Itoh K, et al. Magnetic resonance imaging patterns in patients with multiple myeloma. *Br J Haematol*. 1997; 99:649–655. [PubMed: 9401079]
41. Mouloupoulos LA, Gika D, Anagnostopoulos A, et al. Prognostic significance of magnetic resonance imaging of bone marrow in previously untreated patients with multiple myeloma. *Ann Oncol*. 2005; 16:1824–1828. [PubMed: 16087694]
42. Castellani M, Carletto M, Baldini L, et al. The prognostic value of F-18 fluorodeoxyglucose bone marrow uptake in patients with recent diagnosis of multiple myeloma: a comparative study with Tc-99m sestamibi. *Clin Nucl Med*. 2010; 35:1–5. [PubMed: 20026963]

43. Hillengass J, Wasser K, Delorme S, et al. Lumbar bone marrow microcirculation measurements from dynamic contrast-enhanced magnetic resonance imaging is a predictor of event-free survival in progressive multiple myeloma. *Clin Cancer Res.* 2007; 13:475–481. [PubMed: 17255268]
44. Landgren O, Kyle RA, Pfeiffer RM, et al. Monoclonal gammopathy of undetermined significance (MGUS) consistently precedes multiple myeloma: a prospective study. *Blood.* 2009; 113:5412–5417. [PubMed: 19179464]
45. Weiss BM, Abadie J, Verma P, et al. A monoclonal gammopathy precedes multiple myeloma in most patients. *Blood.* 2009; 113:5418–5422. [PubMed: 19234139]
46. Kyle RA, Remstein ED, Therneau TM, et al. Clinical course and prognosis of smoldering (asymptomatic) multiple myeloma. *N Engl J Med.* 2007; 356:2582–2590. [PubMed: 17582068]
47. Kyle RA, Therneau TM, Rajkumar SV, et al. A long-term study of prognosis in monoclonal gammopathy of undetermined significance. *N Engl J Med.* 2002; 346:564–569. [PubMed: 11856795]
48. Kyle RA, Durie BG, Rajkumar SV, et al. Monoclonal gammopathy of undetermined significance (MGUS) and smoldering (asymptomatic) multiple myeloma: IMWG consensus perspectives risk factors for progression and guidelines for monitoring and management. *Leukemia.* 2010; 24:1121–1127. [PubMed: 20410922]
49. Folkman J, Watson K, Ingber D, et al. Induction of angiogenesis during the transition from hyperplasia to neoplasia. *Nature.* 1989; 339:58–61. [PubMed: 2469964]
50. Rajkumar SV, Mesa RA, Fonseca R, et al. Bone marrow angiogenesis in 400 patients with monoclonal gammopathy of undetermined significance, multiple myeloma, and primary amyloidosis. *Clin Cancer Res.* 2002; 8:2210–2216. [PubMed: 12114422]
51. Rajkumar SV, Leong T, Roche PC, et al. Prognostic value of bone marrow angiogenesis in multiple myeloma. *Clin Cancer Res.* 2000; 6:3111–3116. [PubMed: 10955791]
52. Sezer O, Niemöller K, Eucker J, et al. Bone marrow microvessel density is a prognostic factor for survival in patients with multiple myeloma. *Ann Hematol.* 2000; 79:574–547. [PubMed: 11100749]
53. Munshi NC, Wilson C. Increased bone marrow microvessel density in newly diagnosed multiple myeloma carries a poor prognosis. *Semin Oncol.* 2001; 28:565–569. [PubMed: 11740810]
54. Vacca A, Ribatti D, Roncali L, et al. Bone marrow angiogenesis and progression in multiple myeloma. *Br J Haematol.* 1994; 87:503–508. [PubMed: 7527645]
55. Mouloupoulos LA, Dimopoulos MA, Smith TL, et al. Prognostic significance of magnetic resonance imaging in patients with asymptomatic multiple myeloma. *J Clin Oncol.* 1995; 13:251–256. [PubMed: 7799027]
56. Bellaïche L, Laredo JD, Lioté F, et al. Magnetic resonance appearance of monoclonal gammopathies of unknown significance and multiple myeloma. The GRI Study Group. *Spine (Phila Pa 1976).* 1997; 22:2551–2557. [PubMed: 9383864]
57. Durie BG, Waxman AD, D'Agnolo A, et al. Whole-body (18)F-FDG PET identifies high-risk myeloma. *J Nucl Med.* 2002; 43:1457–1463. [PubMed: 12411548]
58. Hillengass J, Zechmann C, Bäuerle T, et al. Dynamic contrast-enhanced magnetic resonance imaging identifies a subgroup of patients with asymptomatic monoclonal plasma cell disease and pathologic microcirculation. *Clin Cancer Res.* 2009; 15:3118–3125. [PubMed: 19366830]
59. CPT Search. Mar 8. 2011 Available from: [https://catalog.ama-assn.org/Catalog/cpt/cpt\\_search.jsp](https://catalog.ama-assn.org/Catalog/cpt/cpt_search.jsp)

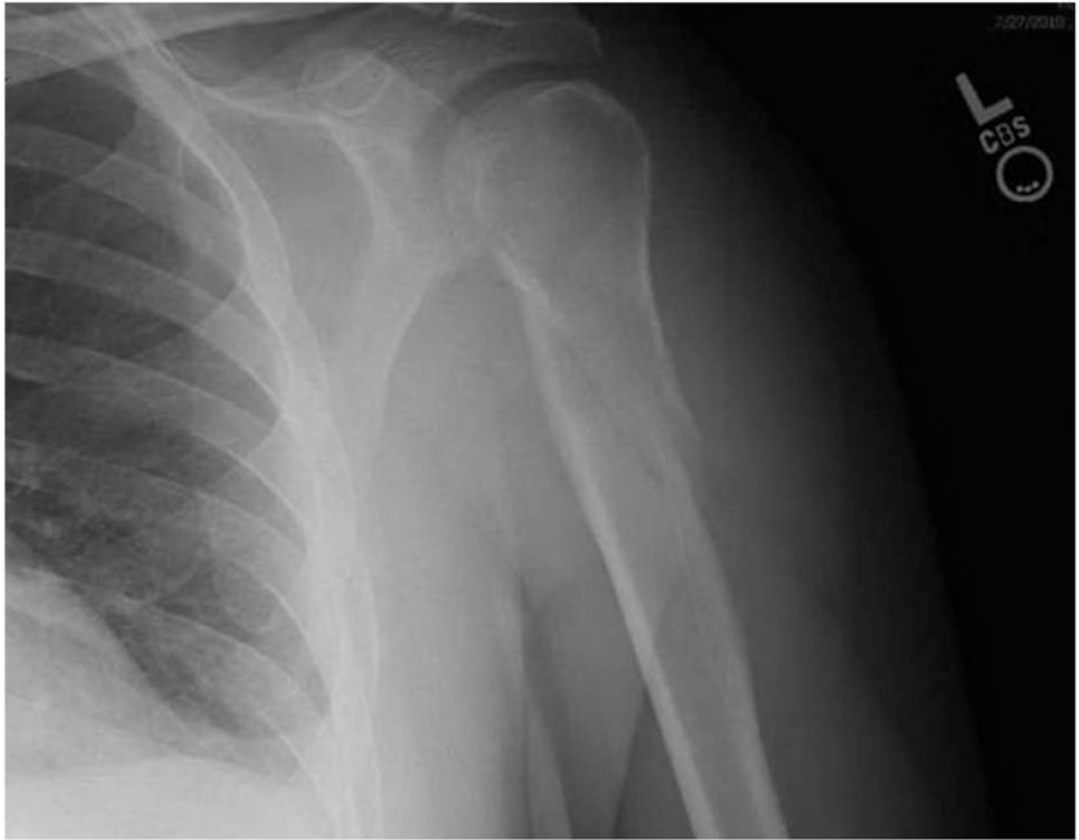


**Figure 1.**  
Plain radiograph of left proximal humerus fracture.



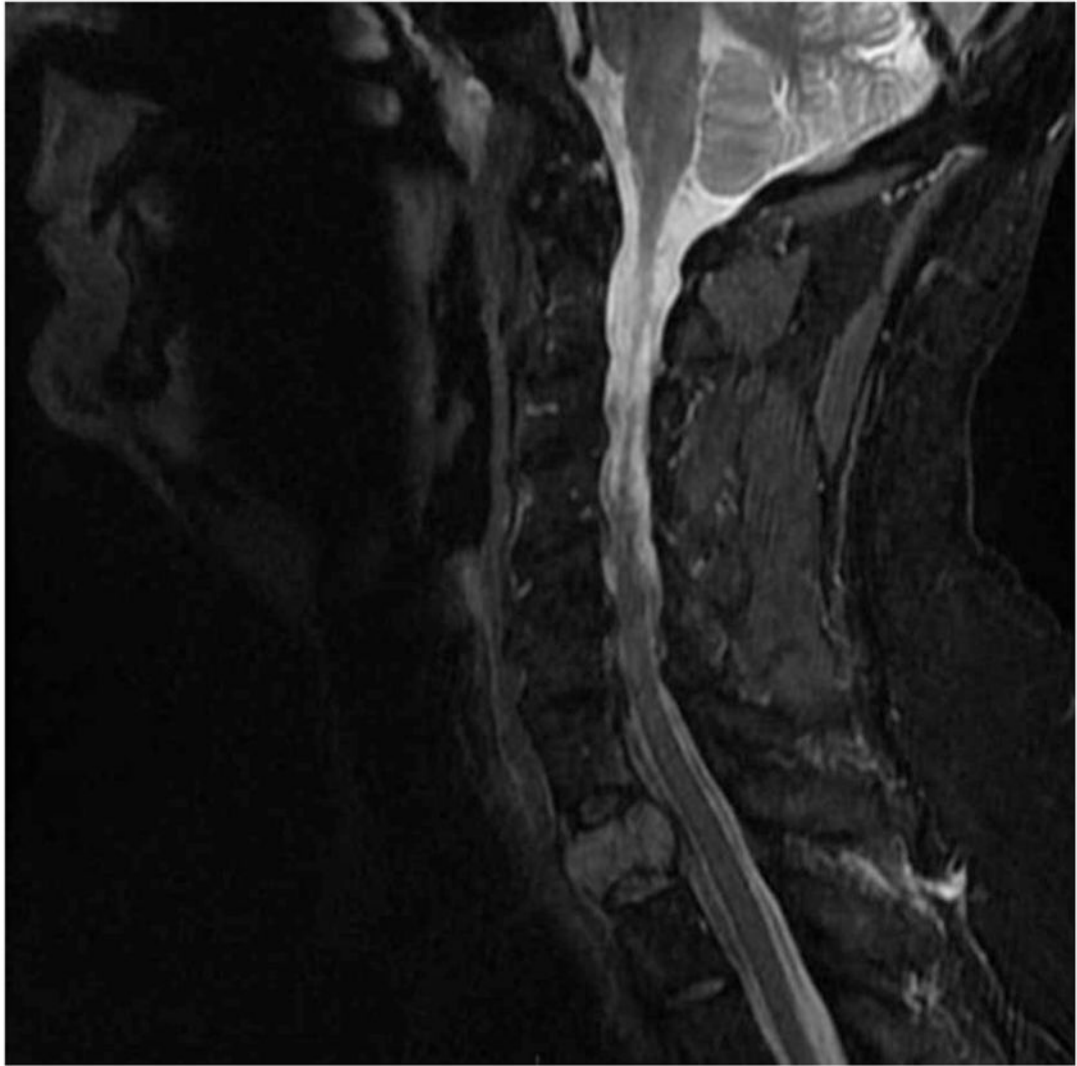


**Figure 2.** MRI scan demonstrates hyperintense signal on T2 weighted MR image in the upper aspect of a thoracic vertebra, consistent with myeloma involvement.

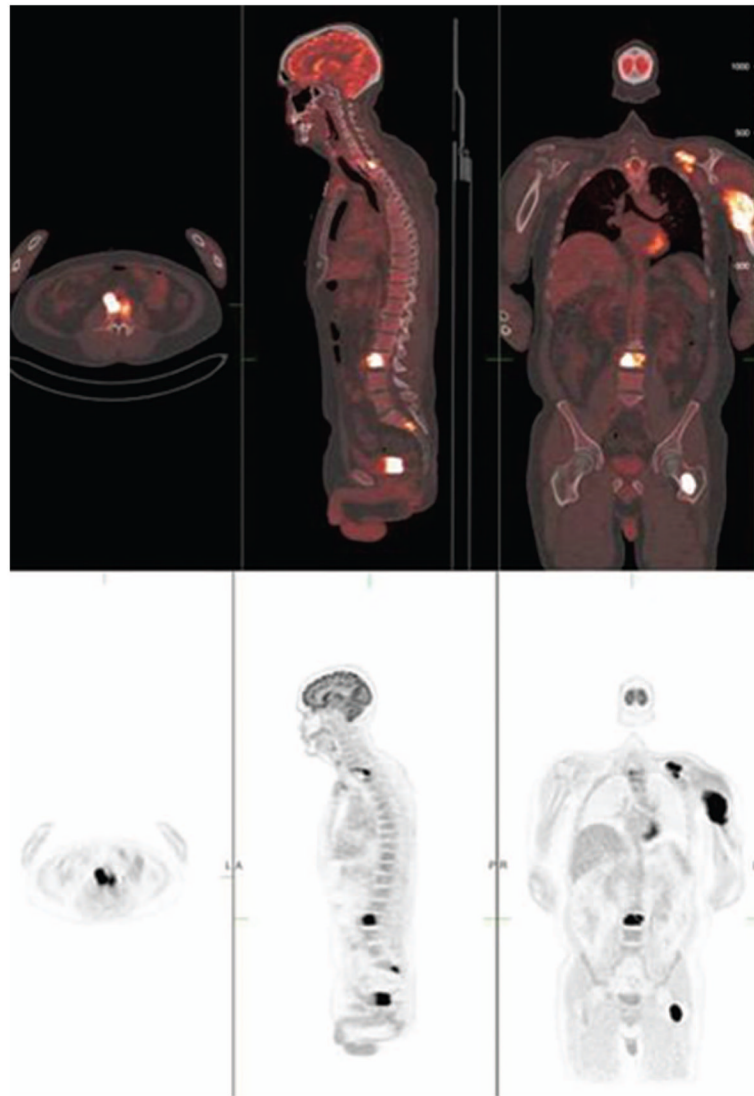


**Figure 3.**  $^{18}\text{F}$ -FDG PET/CT scan demonstrates intense hypermetabolic  $^{18}\text{F}$ -FDG activity in multiple foci, in the left clavicle, left humerus, upper thoracic and lumbar vertebrae, and the proximal aspect of the left femur (bottom row). Combined PET/CT fusion (top row) visualizes both functional and morphologic changes of the multiple bone myeloma involvement.

**Table I**

Features of an optimal imaging modality in multiple myeloma.

---

Widely available
Whole body imaging in one test
Patient comfort
High inter-observer reliability
High sensitivity for the detection of lytic lesions
Ability to detect infiltrative bone marrow focal lesion and extramedullary disease
Ability to assess treatment response
Ability to give prognostic information

---

**Table II**

Comparison of imaging modalities in multiple myeloma.

Modality (radiation exposure)	Radiologic detection of			Advantages	Disadvantages
	Osteolytic lesions	Bone marrow focal lesions	Extramedullary disease		
Skeletal survey (2.1 mSv)	Y	N	N	Widely available Historical standard Low cost	Needs frequent patient repositioning Poor sensitivity, poor quantitation Poor inter-observer reliability Limited areas of visualization
MDCT (25–30 mSv), LDCT (5 mSv)	Y	N	N	Whole body imaging in one test Detects more lytic lesions Provides detailed information on bony involvement in multiple myeloma in anatomically complex regions Widely available Faster scan than standard skeletal survey Provides 3D reconstruction images	High radiation dose exposure in MDCT Low sensitivity in detecting bone marrow involvement or osteopenia
WB-MRI (0 mSv)	Y	Y	Y	Sensitive to bone marrow focal lesions No radiation exposure	Higher cost Prolonged acquisition time Problematic in patients with metallic objects in their body May not be widely available Inferior to MDCT in the detection of bone lesions
<sup>18</sup> F-FDG PET/CT (14–16 mSv)	Y	Y	Y	Detects extramedullary disease Detects focal bone marrow lesions Whole body imaging in one test Able to distinguish benign vs. malignant findings	Tracer not always available High cost Limited detection of sub-centimeter lesions Detects areas of inflammation and infection
<sup>18</sup> F-NaF PET/CT (14–16 mSv)	Y	Y	Y	Preferentially concentrates at malignant sites Sensitive to osteoblastic and osteolytic activity	Tracer not widely available Limited studies available
<sup>99m</sup> Tc-sestamibi (6.2 mSv)	N	Y	N	Able to detect focal bone marrow lesions	Limited sensitivity Underestimates degree of BM infiltration in low stage disease
<sup>11</sup> C-methionine PET/CT (14 to 16 mSv)	Y	Y	Y	Detects extramedullary disease Detects focal bone marrow lesions Whole body imaging in one test Able to detect osteolytic lesions	Tracer not widely available Limited studies

MDCT, multidetector computed tomography; LDCT, low dose CT; WB-MRI, whole body magnetic resonance imaging; <sup>18</sup>F-FDG PET/CT, fluorine-18 fluorodeoxyglucose positron emission tomography CT; <sup>18</sup>F-NaF PET/CT, fluorine-18 sodium fluoride PET/CT; BM, bone marrow.